Eur. Phys. J. B **38**, 169–175 (2004)
DOI: 10.1140/epjb/e2004-00022-4

THE EUROPEAN PHYSICAL JOURNAL B

Hot spots and universality in network dynamics

A.-L. Barabási[1], M.A. de Menezes[1,a], S. Balensiefer[2], and J. Brockman[2]

[1] Department of Physics, University of Notre Dame, Notre Dame, IN 46556, USA
[2] Department of Computer Science and Engineering, University of Notre Dame, Notre Dame, IN 46556, USA

Received 25 October 2003
Published online 17 February 2004 –

Abstract. Most complex networks serve as conduits for various dynamical processes, ranging from mass transfer by chemical reactions in the cell to packet transfer on the Internet. We collected data on the time dependent activity of five natural and technological networks, finding evidence of orders of magnitude differences in the fluxes of individual nodes. This dynamical inhomogeneity reflects the emergence of localized high flux regions or "hot spots", carrying an overwhelming fraction of the network's activity. We find that each system is characterized by a unique scaling law, coupling the flux fluctuations with the total flux on individual nodes, a result of the competition between the system's internal collective dynamics and changes in the external environment. We propose a method to separate these two components, allowing us to predict the relevant scaling exponents. As high fluctuations can lead to dynamical bottlenecks and jamming, these findings have a strong impact on the predictability and failure prevention of complex transportation networks.

PACS. 89.75.-k Complex systems – 89.75.Da Systems obeying scaling laws – 05.40.-a Fluctuation phenomena, random processes, noise, and Brownian motion

1 Introduction

Research on the structure of complex networks has greatly benefited from the availability of detailed topological maps describing various complex systems [1]. Yet, advances in uncovering the mechanisms shaping the topology of complex networks [2–5] are overshadowed by our lack of understanding of common organizing principles governing network dynamics. Focusing on the dynamics of few selected nodes resulted in a series of important discoveries, such as self-similar traffic patterns on Internet routers [6–9] or long range correlations in biological or economic time series [10,11] have been made. Less is known, however, about how the collective behavior of often millions of nodes contribute to the observable dynamical features of a complex system. In particular, we continue to search for dynamical organizing principles that are common to a wide range of complex networks. To succeed, we need to complement the topological maps of complex networks with data on the time resolved activity of each node and link. Indeed, to uncover a cell's dynamical behavior we must access the time dependent concentrations of hundreds of proteins and metabolites, or to study the dynamics of the Internet we must monitor traffic simultaneously on hundreds of thousand routers.

[a] e-mail: mdemenez@nd.edu

2 Quantifying network dynamics on real systems

In complex dynamical systems with many components (nodes) each node i is characterized by a time dependent variable $f_i(t)$ $(i = 1, \ldots, N)$ (as $f_i(t)$ often describes transport across node i, we will refer to it as flux). Even within the same system the flux on different nodes can differ widely. For example, both the average traffic $\langle f_i \rangle = 1/T \sum_{t=1\ldots,T} f_i(t)$ and the fluctuations about the average $\sigma_i = \sqrt{\langle f_i^2 \rangle - \langle f_i \rangle^2}$ of four Internet routers on the same network differ by orders of magnitude (Fig. 1a). Natural systems, such as highway networks, show similar characteristics: both the average traffic on a given highway and traffic fluctuations span several orders of magnitude on different points of a highway network (Fig. 1b).

To quantify these visually apparent flux differences for four complex networks we recorded the relevant dynamical variable $f_i(t)$ over an extended time interval from hundreds to thousands of accessible nodes. We find that for each of these systems the time averaged flux $\langle f_i \rangle$ on different nodes spans four (microchip, Fig. 3c) to six (Internet, Fig. 3a) orders of magnitude, leading to a wide $P(\langle f \rangle)$ flux distribution. The wide range of $\langle f \rangle$ values indicate that while most nodes have relatively small fluxes, in each system there are groups of nodes for which $\langle f \rangle$ takes extraordinary large values, orders of magnitude higher than

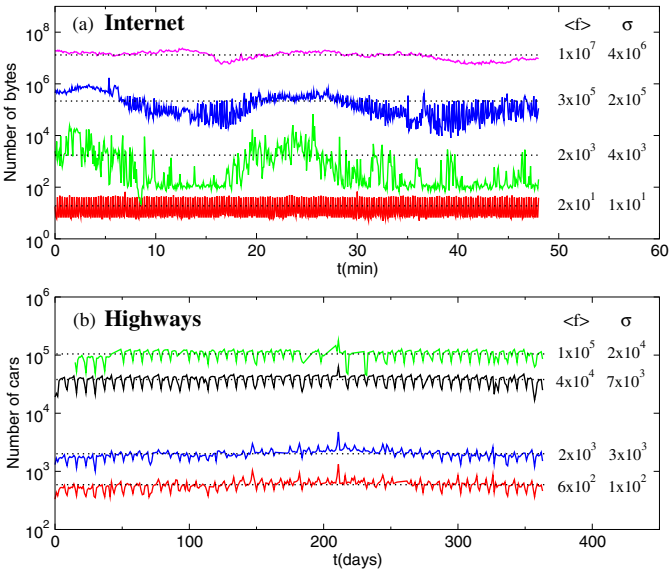

Fig. 1. The dynamics of a few individual nodes of the Internet. Time dependent traffic on four Internet routers of the Mid-Atlantic Crossroads (MAX) network (`http://www.maxgigapop.net`), whose activity is monitored by the Multi Router Traffic Grapher software (`http://people.ee.ethz.ch/~oetiker/webtools/mrtg/`). The figure shows the number of bytes per second for each of the routers in five minutes intervals for a two day period. (b) Average traffic on four different Colorado highways segments, measured in number of cars per second in the year of 2001. Traffic recorded in hourly resolution by the US Department of Transportation (`http://dot.state.co.us`). On the right of both plots we show the time average of the flux $\langle f \rangle$ displayed as horizontal dotted lines superposed on the graphs, and the dispersion, σ, for each of the shown signals, indicating orders of magnitude differences in both flux and dispersion between nodes of the same network.

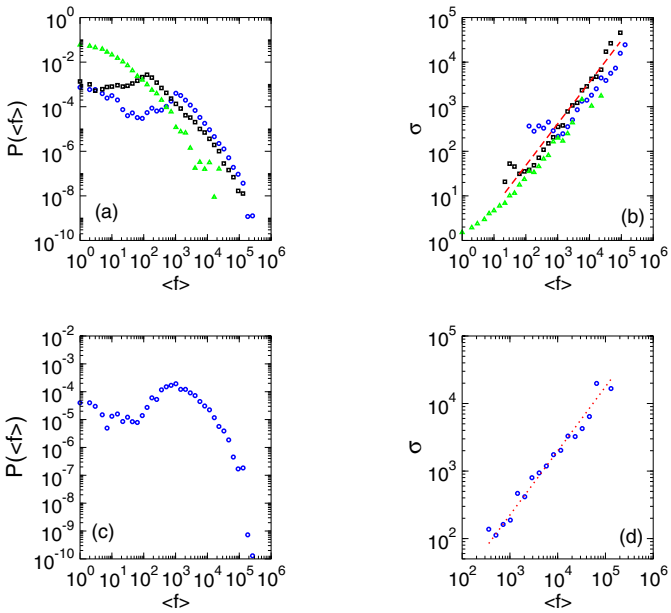

Fig. 2. Characterizing systems belonging to the driven ($\alpha = 1$) universality class. (a, b): Daily visitations on several thousand websites were collected using the Nedstat (http://www.nedstatbasic.net) web monitor, which keeps track of the daily access to thousands of web pages. We analyzed daily traffic on each web page for a 30 day period, calculating the average flux for 1,000 sites on USA (blue circles), 1,000 on Brazil (black squares) and 1,000 on Japan (green triangles). In (a) we show the distribution of the average visitation $\langle f \rangle$ for each of the monitored web sites, the common envelope of the curves suggesting an asymptotic power-law behavior. The drop in $P(\langle f \rangle)$ for small $\langle f \rangle$ reflects the fact that for each country we have access only to the 1,000 most visited sites, thus the less visited small $\langle f \rangle$ sites are undersampled. On (b) we show the dependence of the dispersion on the average flux, measured for each of the nodes separately. (c, d): Daily traffic on Colorado and Vermont highways, provided by the Colorado Department of Transportation and Vermont Agency of Transportation, respectively (`http://dot.state.co.us` and `http://aot.state.vt.us`). We used the data on the daily number of cars passing through observation points on 127 highways from 1998 to 2001 to determine the average flux distribution (c), as well as the relationship between the dispersion and flux (d). The drop in $P(\langle f \rangle)$ for small $\langle f \rangle$ again likely reflects the incomplete sampling of the small traffic roads. In (b) and (d) the red dashed line has slope $\alpha = 1$.

the flux on typical nodes, generating highly active regions, or "hot spots". These hot spots are responsible for a considerable fraction of the system's activity: in the Internet we find that the top 20% of the nodes carry 95% of total traffic. A similar unbalance is present in all studied systems, our measurements indicating that the top 20% of nodes carry 73%, 76% and 54% of the activity on the World Wide Web, highways and computer chip, respectively. While the existence of such high flux regions is a well known problem in Internet traffic [12–14], their emergence in each of the studied systems suggests that hot spots are a generic feature of transport on complex networks. Indeed, such wide link strength distributions have been observed lately in a wide range of systems, from stock markets [15] to metabolic networks [16].

Traditional dynamical approaches to complex systems focus on the long time behavior of at most a few dynamical variables, characterizing either a single node or the system's average behavior. To simultaneously characterize the dynamics of thousands of nodes we focus on the coupling between the average flux and the fluctuations around the average. In many dynamical systems the time average $\langle f \rangle$ of the relevant dynamical variable, $f(t)$, and its fluctuations around the average, σ, are decoupled. Consider for example an unbiased random walker, for which the fluctuations around the average position increase as $\sigma \sim t^{1/2}$, while its average position $\langle f \rangle$ is independent of time, resulting in a decoupling between $\langle f \rangle$ and σ [17,18]. In contrast, our measurements indicate that in complex networks there is a characteristic coupling between the average flux $\langle f_i \rangle$ and dispersion σ_i of individual nodes (Fig. 1). To quantify this observation we plot σ_i for each node i in function of the average flux $\langle f_i \rangle$ of the same node (Figs. 2 and 3). We find that for four systems for which

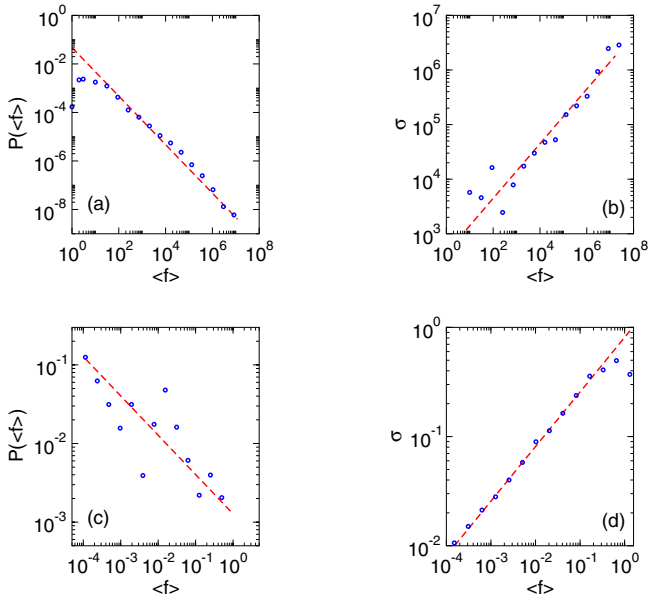

Fig. 3. Characterizing systems belonging to the endogenous ($\alpha = 1/2$) universality class. (a, b): We collected time resolved information for 374 Internet links of the Mid-Atlantic Crossroads (MAX) (`http://www.maxgigapop.net`) and the ABILENE (`http://www.abilene.iu.edu`) networks, MIT routers (`http://web.mit.edu/mrtg/www`), UNAM routers (`ww.unam.edu.ar/mrtg`), all Brazilian RNP backbones (`http://www.rnp.br`), and dozens of smaller routers on the Internet, obtaining for each link two days of activity with five minute resolution. The distribution of the average fluxes (a) indicates a power-law dependence $P(\langle f\rangle) \sim \langle f\rangle^{-1}$, while the dependence of the dispersion on the flux for individual nodes (b) indicates $\alpha^I = 1/2$. (c, d): The activity on of the 462 signal carriers of the 12-bit Simple12 microprocessor, recorded and analyzed when the processor is given the task of finding the smallest number of an array, requiring 8,862 clock cycles. At each clock cycle each signal carrier is either active $f = 1$ or inactive $f = 0$. The flux distribution (c) can be approximated with a power-law $P(\langle f\rangle) \sim \langle f\rangle^{-0.7}$, and the dependence of the dispersion on the flux for the individual nodes (d) again follows $\alpha^m = 1/2$.

extensive dynamical data is available the dispersion depends on the average flux as

$$\sigma \sim \langle f\rangle^{\alpha} . \qquad (1)$$

Most intriguing, however, is the finding that for the studied systems the dynamical exponent α is in the vicinity of two distinct values, $\alpha = 1$ (Fig. 2) and $\alpha = 1/2$ (Fig. 3), suggesting that diverse real systems can display two distinct dynamical behaviors [19]. Next we discuss the evidence for each of these systems separately.

The $\alpha \simeq 1$ systems (Fig. 2): The WWW, an extensive information depository, is a network of documents linked by URLs [20–23]. As many websites record individual visits, surfers collectively contribute to a dynamical variable $f_i^w(t)$ that represents the number of visits page i receives during day t. We studied the daily breakdown of visitation for 30 days for 3,000 sites scattered over three continents, determining for each node i the average $\langle f_i^w\rangle$ and dispersion σ_i^w. As Figure 2 shows, σ_i^w and $\langle f_i^w\rangle$ follow (1) over five orders of magnitude with dynamical exponent $\alpha^w = 1$. The highway system is an example of a transportation network, the relevant dynamical variable being the traffic at different locations. We analyzed the daily breakdown of traffic measurements at 127 locations on Colorado and Vermont highways. The results, shown in Figure 2f, again document a strong coupling between $\langle f_i^h\rangle$ and σ_i^h, the scaling spanning over five orders of magnitude indicating $\alpha^h = 1$.

The $\alpha \simeq 1/2$ systems (Fig. 3): The Internet, viewed as a network of routers linked by physical connections, serves as a transportation network for information, carried in form of packets [24–27]. Daily traffic measurements of 374 geographically distinct routers indicate that while the relationship between traffic and dispersion follows (1) for close to seven orders of magnitude, in contrast with the previous systems we have $\alpha^I = 1/2$ (Fig. 3b). In a microprocessor, in which the connections between logic gates generate a static network, information is carried in the form of electric currents [28]. At each clock cycle a certain subset of connections i are active, the relevant dynamical variable $f_i(t)$ taking two possible values, 0 or 1. The activity during 8,862 clock cycles on 462 nodes of the Simple12 microprocessor indicates that the average flux and fluctuations follow (1), with $\alpha^m = 1/2$ (Fig. 3d). The distinct nature of the exponents and the quality of scaling documented in Figures 2 and 3 indicate the existence of common organizing principles across different network topologies.

3 Modelling network dynamics – Internal dynamics vs. external fluctuations

To understand the origin of the observed dynamical scaling law (1) we study a simple dynamical model that incorporates some key elements of the studied systems. While the topology of these systems vary widely, from exponential (highway network) to a scale-free network (WWW, Internet), a common feature of the studied systems is the existence of a transportation network that channels the flux toward selected nodes. Therefore, we start with a network of N nodes and L links, described by an adjacency matrix M_{ij}, which we choose to describe either a scale-free or a random network [29,30]. As the dynamics of the studied systems varies widely, we study two different dynamical rules. *Model 1* considers the random diffusion of W walkers on the network, such that each walker that reaches a node i departs in the next time step along one of the links the node has. Each walker is placed on the network at a randomly chosen location and removed after it performs M steps, mimicking in a highly simplified fashion a human browser surfing the Web for information. To probe the collective transport dynamics counters attached to each node record the number of visits by individual walkers. To capture the day to day fluctuations on individual nodes we repeat the diffusion of W walkers D times on a fixed network and denote by $f_i(t)$ the number of visits to node i on day $t = 1, \ldots, D$. As Figure 4a

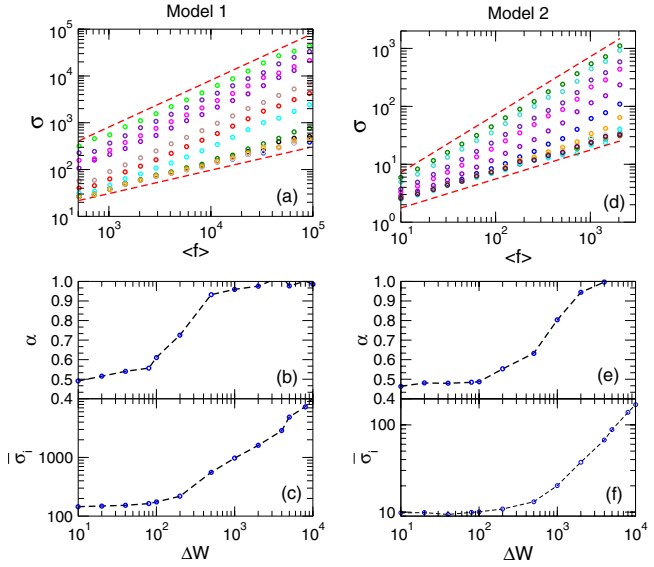

Fig. 4. Modeling network dynamics. To understand the interplay between the internally and the externally driven dynamics we studied the dynamics of two models on a scale-free network [4] with $\gamma = 3$ and 10^4 nodes. In Model 1 on each "day" t we release $W(t) = \langle W \rangle + \xi(t)$ walkers on random positions of the network, and allow each of them to perform $M = 10^3$ random diffusive steps along the network, where $\xi(t)$ is a uniformly distributed random variable between $-\Delta W$ and ΔW and $\langle W \rangle = 10^4$. For each node i we record the number of times it has been visited by a walker, $f_i(t)$, repeating the same procedure for $t = 30$ days. Note that longer t runs generate identical results. The time average of $f_i(t)$ provides $\langle f_i \rangle$, and allows us to study the relation between the average flux $\langle f_i \rangle$ and fluctuations about the average σ_i. (a) The figure shows the $\sigma(\langle f \rangle)$ curves for $\Delta W = 0, 10, 20, 40, 80, 100, 200, 500, 1000, 2000, 4000, 5000$ and 10000 from top to bottom, demonstrating a crossover between the $\sigma \sim \langle f \rangle^{1/2}$ ($\alpha = 1/2$) and $\sigma \sim \langle f \rangle$ ($\alpha = 1$) behavior as ΔW increases. (b) The dependence of the exponent α on W, obtained by fitting the σ_i versus $\langle f_i \rangle$ curves shown in (a) for different values of ΔW. Note that while the figure shows a gradual transition, most likely the intermediate α values represent finite size effects, and the transition in infinite systems should be sharp between $\alpha = 1/2$ and 1. (c) Average fluctuations $\langle \sigma_i \rangle$, obtained by averaging σ_i over all nodes i in the system, shown in function of the amplitude of the external driving force ΔW. While under $\Delta W \approx 10^3$ the magnitude of $\langle \sigma_i \rangle$ is independent of ΔW, for large ΔW the fluctuations increase rapidly with ΔW, indicating that the network dynamics is externally driven. (d–f) The same as in (a–c), but for Model 2, where the diffusive dynamics was replaced by message passing. In the model, each "day" t we choose W pairs of nodes, sending a message between them along the shortest path. W was again chosen from an uniform distribution of width ΔW and average $\langle W \rangle = 10^4$.

indicates, the average flux and fluctuations follow (1) with $\alpha = 1/2$. Similar results are obtained for *Model 2*, in which we replaced the random diffusive dynamics with a directed flow process. In this case each day t we pick W randomly selected pairs of nodes, designating one node as a sender and the other as a recipient, and send a message between them along the shortest path. Counters placed on each node count the number of messages passing through. This dynamics mimics, in a highly schematic fashion, the low density traffic between two nodes on the Internet. As Figure 4d shows, we find that Model 2 also predicts $\alpha = 1/2$, indicating that the $\alpha = 1/2$ exponent is not a particular property of the random diffusion model, but it is shared by several dynamical rules.

We can understand the origin of the $\alpha = 1/2$ exponent if we inspect the origin of fluctuations in Model 1. In the $M = 1$ limit walkers arrive to randomly selected nodes but fail to diffuse further, reducing the dynamics to random deposition, a well known model of surface roughening [31,32]. Therefore, the average visitation on each node grows linearly with time, $\langle f \rangle \sim t$, and the dispersion increases as $\sigma \sim t^{1/2}$, providing $\alpha = 1/2$ [31,32]. If $M > 1$, since the connections between nodes are random, one can still interpret the random arrival of walkers and further diffusion as a random deposition process [33], each node i receiving a fraction $r_i \propto k_i$ of the total number of steps $W \times M$ performed on the network, and the average visitation $\langle f_i \rangle$ again scaling with fluctuations σ_i as $\langle f_i \rangle \sim \sigma_i^{1/2}$.

Real systems are often exposed to changes in the external environment that makes the amount of material flowing through the network to vary. To incorporate the effect of such externally induced fluctuations we allow W, which represents the number of walkers in Model 1 and the number of messages in Model 2, to vary from one day to the other. Assuming that the day to day variations of $W(t)$ are a dynamic variable randomly chosen from an uniform distribution in the interval $[W - \Delta W, W + \Delta W]$, we recover $\alpha = 1/2$ for $\Delta W = 0$. However, when ΔW exceeds a certain (model dependent) threshold, in both models the dynamical exponent changes to $\alpha = 1$ (Figs. 4b and e).

To understand the origin of the $\alpha = 1$ exponent we notice that on each node the observed day to day fluctuations have two sources. For $\Delta W = 0$ we have only internal fluctuations, coming from the fact that under random diffusion (or random selection of senders and receivers in Model 2) the number of walkers (messages) that pass by a certain node fluctuates from day to day. For $\Delta W \neq 0$ the fluctuations have an external component as well, as when the total number of walkers (messages) change from one day to the other, they proportionally alter the visitation of the individual nodes as well. If the magnitude of the day to day fluctuations is significant, they can overshadow the internal fluctuations σ_i^{int}. Indeed, if in a given time frame the total number of walkers or messages doubles, the flux on each node is expected to grow with a factor of two, a change that could be much larger than changes induced by potential internal fluctuations. Therefore, for $\Delta W \neq 0$ the external driving force, determined by the time dependent $W(t)$, contributes to the daily fluctuations with a dispersion $\sigma^{dr}(\Delta W) = \sqrt{\langle W(t)^2 \rangle - \langle W(t) \rangle^2}$, which is a monotonic function of ΔW. The total fluctuations for node i are therefore given by $\sigma_i = \sigma_i^{int} + \sigma_i^{ext}$, where $\sigma_i^{ext} = A_i \sigma^{dr}(\Delta W)$, A_i being a geometric factor capturing the fraction of walkers channeled to node i, and depends only on the position of node i within the network.

When $\Delta W = 0$, the external component σ^{dr} vanishes, resulting in $\sigma_i^{int} = a_i \langle f_i \rangle^{1/2}$, as discussed earlier. When ΔW is sufficiently large, so that $A_i \sigma^{dr}(\Delta W) \gg \sigma_i^{int}$, then the fluctuations are dominated by the changes in the external driving force, allowing us to approximate the flux at node i with $f_i(t) = A_i W(t)$. In this case we have $\langle f_i \rangle = A_i \langle W(t) \rangle$ and $\langle {f_i}^2 \rangle = {A_i}^2 \left\langle W(t)^2 \right\rangle$, giving $\sigma_i = \sqrt{\langle {f_i}^2 \rangle - \langle f_i \rangle^2} = A_i \sigma^{dr}$. As σ^{dr} and $\langle W(t) \rangle$ are time independent characteristics of the external driving force, we find $\sigma_i = \sigma_i^{ext} = \frac{\sigma^{dr}}{\langle W(t) \rangle} \langle f_i \rangle$, providing the observed coupling (1) with $\alpha = 1$. Note that this derivation is independent of the network topology or the details of the particular transport process, predicting that any system for which the magnitude of fluctuations in the external driving force exceeds the internal fluctuations will be characterized by (1) with an $\alpha = 1$ exponent.

These calculations imply that the fluctuations on a given node can be decomposed into an internal and an external component as

$$\sigma_i = a_i \langle f_i \rangle^{1/2} + \frac{\sigma^{dr}}{\langle W(t) \rangle} \langle f_i \rangle . \tag{2}$$

Therefore, gradually increasing the amplitude of fluctuations ΔW in the studied models we should induce a change from the $\alpha = 1/2$ intrinsic or endogenous to the $\alpha = 1$ driven behavior. To confirm the validity of this prediction, in Figures 4c and f we show the average fluctuation $\bar{\sigma}_i$ over all nodes in function of the amplitude ΔW of the driving force. For both models we find that for small ΔW values $\bar{\sigma}_i$ remains unchanged, as in this regime $\bar{\sigma}_i \sim \sigma_i^{int} > \sigma_i^{ext}$, independent of ΔW. However, after ΔW exceeds a certain threshold, $\bar{\sigma}_i$ rapidly increases with ΔW. In this second regime the fluctuations are driven by external forces, $\bar{\sigma}_i \sim \sigma_i^{ext} \sim \bar{A}_i \sigma^{dr}$, and according to (2) we should observe $\alpha = 1$. Indeed, we find that in both models the transition from the constant to the increasing $\bar{\sigma}_i$ (Figs. 4c, f) coincides with the crossover from the $\alpha = 1/2$ to the $\alpha = 1$ regime (Figs. 4b, e). To understand to what degree our findings depend on the specific simulation and model details we altered most assumptions in both models, changing the topology from scale-free to random networks and from undirected to directed networks, as well as altering the nature of the external fluctuations by keeping W constant in Model 1 but forcing the number of steps, M, to play the role of the stochastic external driving force. For each modified version of the models we recover the transition between the $\alpha = 1/2$ and $\alpha = 1$ behavior when the amplitude of the external fluctuations exceeds a certain threshold.

4 Separating internal and external contributions to network dynamics

The results of the previous section indicate that two different mechanisms are responsible for the flux fluctuations in complex networks. The $\alpha = 1/2$ exponent captures an endogenous behavior, characterizing the system's internal collective fluctuations. In contrast, the $\alpha = 1$ exponent indicates that the fluctuations of individual nodes are driven by time dependent changes in the external forces. To connect this prediction with the empirical results, next we introduce a method that allows us to separate the intrinsic and the external fluctuations in the experimental data. We start by separating the dynamical variable $f_i(t)$ into two components,

$$f_i(t) = f_i^{int}(t) + f_i^{ext}(t), \tag{3}$$

the first describing the contribution from the internal dynamics, the second being the externally driven component.

To determine $f_i^{ext}(t)$ let us consider the case when internal fluctuations are absent, and therefore the total traffic in the system is distributed in a deterministic fashion among all components. In this case component i captures a time independent fraction A_i of the total traffic. For different components i, A_i can differ significantly, being determined by the component's centrality [34]. The challenge is to extract A_i from the experimentally available data without knowledge of the system's internal topology or the dynamical rules governing its activity. For this we write A_i as the ratio of the total traffic going through the component i in the time interval $t \in [0, T]$ and the total traffic going over all observed components during the same time interval

$$A_i = \frac{\sum_{t=1}^{T} f_i(t)}{\sum_{t=1}^{T} \sum_{i=1}^{N} f_i(t)}. \tag{4}$$

At any moment t the amount of traffic *expected* to go through node i is therefore given by the product of A_i and the total traffic in the system in moment t (i.e. $\sum_{i=1}^{N} f_i(t)$), providing the magnitude of the traffic expected if only external fluctuations contribute to the activity of node i as

$$f_i^{ext}(t) = A_i \sum_{i=1}^{N} f_i(t). \tag{5}$$

Equation (5) describes the case in which changes in the system's overall activity are reflected in a proportional fashion on each component. Real systems do display, however, internal fluctuations, which will generate local and temporal deviations from the expected $f_i^{ext}(t)$, a consequence of the internal time dependent redistribution of traffic in the system. Using $(1-3)$ we obtain this internal component as

$$f_i^{int}(t) = f_i(t) - \left(\frac{\sum_{t=1}^{T} f_i(t)}{\sum_{t=1}^{T} \sum_{i=1}^{N} f_i(t)} \right) \sum_{i=1}^{N} f_i(t), \tag{6}$$

which, by definition, has zero average, as it captures the deviations from the traffic expected to go through component i. Given the experimentally measured dynamic signal $f_i(t)$ on a large number of components, (5) and (6) allow us to separate each signal $f_i(t)$ into two contributions $f_i^{ext}(t)$ and $f_i^{int}(t)$, the first capturing changes in the system's overall activity, providing a measure of the external fluctuations and the second describing the fluctuations characterizing the system's internal dynamics.

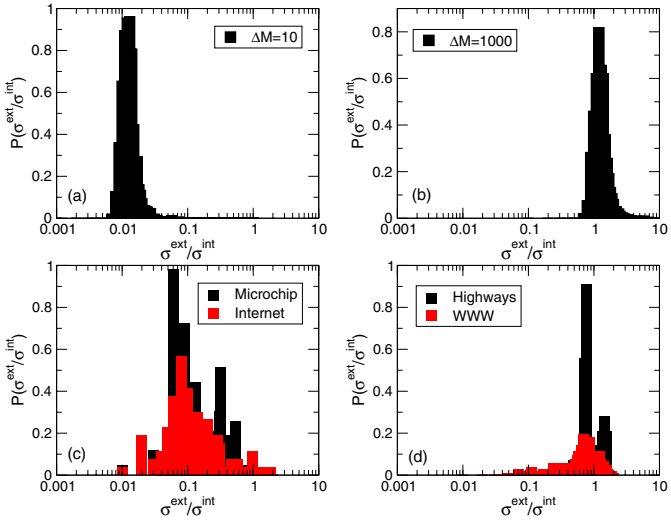

Fig. 5. Distribution of $\eta_i = \sigma_i^{ext}/\sigma_i^{int}$ ratios of external and internal fluctuations for model (a, b) and selected real systems **(c,d)**. Distribution of the η_i ratios for the random walk model: (a) For smaller external fluctuations, the distribution is centered around a small value of $\eta \ll 1$, indicating that internal fluctuations overcome external ones, dominating the system's dynamics. (b) When ΔM is increased, however, such fluctuations overshadow the system's internal dynamics, and the $P(\eta)$ distribution shifts towards larger values of η (right curve). (c) $P(\eta)$ distributions for the Internet and the microchip, centered around $\eta \sim 0.1$, indicate that external fluctuations do not affect the system's overall dynamics significantly. (d) The World Wide Web and the Highway networks, with $P(\eta)$ peaked around $\eta \sim 1$, are strongly influenced by fluctuations in the total number of web surfers and the number of cars, respectively.

From $f_i^{int}(t)$ and $f_i^{ext}(t)$ we can calculate $\eta_i = \sigma_i^{int}/\sigma_i^{ext}$ for each node, and from that the $P(\eta)$ distribution, which gives a measure of the impact of external fluctuations on the internal dynamics of the system. Indeed, as we vary ΔM towards larger values in the model, we obtain that the $P(\eta)$ curve also shifts towards larger $\sigma_i^{int}/\sigma_i^{ext}$ ratios (Figs. 5a–b).

Doing the same analysis on the empirical systems, we find that majority of nodes for the Internet and the computer chip (for which $\alpha \simeq 1/2$) have $\sigma_i^{int}/\sigma_i^{ext} \ll 1$ (Fig. 5c), indicating that internal fluctuations dominate over external ones. In contrast, for systems displaying the $\alpha \simeq 1$ exponent (WWW, highway) the $P(\eta)$ curve is centered about $\eta \sim 1$ (Fig. 5d), indicating that external and internal fluctuations are comparable. These results offer experimental support to our earlier findings that the dynamical exponent α is determined by the relative magnitude of the external and internal fluctuations in both the model and empirical systems.

5 Conclusions

The wide range of $\langle f_i \rangle$ values, as captured by the broad $P(\langle f_i \rangle)$ distribution, indicates that in transportation networks a few nodes emerge as hot spots with exceptionally high fluxes. To avoid bottlenecks or slowdown induced failures in transportation networks, the capacity of the individual nodes must be adjusted to accommodate these high flux regions [12,13], each node's capacity exceeding the expected maximum flux on that node [35]. There are significant differences, however, in our ability to predict the maximal flux for systems driven by internal or external fluctuations. An important quantity for predicting the potential demand on a given node i is the relative fluctuation, $w_i = \sigma_i / \langle f_i \rangle$. For $\alpha = 1/2$ we have $w \sim \langle f \rangle^{-1/2}$, i.e. the relative fluctuations decrease for the critical high flux nodes. Therefore, these systems require less resources on the hot spots, and carry less risk for breakdowns due to fluxes that temporarily exceed the node's capacity. This is good news for the Internet and the computer chip, as the $\alpha = 1/2$ exponent indicates that one can offer reasonable bounds on the maximum capacity, potentially avoiding bottlenecks. In contrast, for driven systems ($\alpha = 1$) w is independent of flux, i.e. fluctuations on the hot spots increase linearly with the flux. To accommodate temporary flux peaks, the capacity of the high flux nodes needs to be significantly higher than the average flux. Therefore, the maximum number of visitors on popular websites or the maximal traffic on some highways is expected to vary widely, requiring significant infrastructural investments to avoid accidental bottlenecks and challenging our ability to plan for maximal usage.

A wide range of complex networks, from the cell [36–40] to economic systems [41–43], support rapidly fluctuating transport processes, such as chemical reactions in the cell or monetary transfers in the economy. Our results indicate that the relative magnitude of these fluctuations depends on the system's collective dynamics and is captured by the dynamical exponent α, which in turn is determined by the relative magnitude of the external and internal fluctuations. Distinguishing between intrinsic and extrinsic noise has been found useful in gene expression [44,45], and localized high activity regions are encountered in random resistor networks [46–49] and the Internet [14]. Our results indicate that these are not isolated system specific findings, but represent signatures of dynamic mechanisms that are common for a wide range of complex networks.

We are indebted to János Kertész for fruitful discussions. This research was supported by grants from NSF, NIH and DOE.

References

1. The Cooperative Association for Internet Data Analysis (`http://www.caida.org`), BioCyc Knowledge Database (`http://biocyc.org`), Yeast Protein Complex Database (`http://yeast.cellzome.com`) and others
2. *Handbook of Graphs and Networks*, edited by S. Bornholdt, H.G. Schuster (Wiley-VCH, Berlin, 2002)
3. S.N. Dorogovtsev, J.F.F. Mendes, Adv. Phys. **51**, 1079 (2002)

4. R. Albert, A.-L. Barabási, Rev. Mod. Phys. **74**, 47 (2002)
5. S.H. Strogatz, Nature **410**, 268 (2001)
6. W.E. Leland, M.S. Taqqu, W. Willinger, D.V. Wilson, IEEE/ACM Trans. Networking **2**, 1 (1994)
7. M. Crovella, A. Bestavros, IEEE/ACM Trans. Networking **5**, 835 (1997)
8. I. Csabai, J. Phys. A **27**, L417 (1994)
9. K. Fukuda, M. Takayasu, H. Takayasu, Physica A **287**, 289 (2000)
10. A.L. Goldberger, L.A.N. Amaral, J.M. Hausdorff, P.C. Ivanov, C.K. Peng, H.E. Stanley, Proc. Natl. Acad. Sci. USA **99**, 2466 (2002)
11. R.N. Mantegna, H.E. Stanley, Nature **376**, 46 (1995)
12. K.-I. Goh, B. Kahng, D. Kim, Phys. Rev. Lett. **87**, 278701 (2001)
13. K.-I. Goh, E.S. Oh, H. Jeong, B. Kahng, D. Kim, Proc. Natl. Acad. Sci. USA **99**, 12583 (2002)
14. S. Uhlig, O. Bonaventure, Technical Report Infonet-TR-10, University of Namur, June 2001 `http://www.infonet.fundp.ac.be/doc/tr/Infonet-TR-2001-10.html`
15. D. Garlaschelli, S. Battiston, M. Castri, Vito D.P. Servedio, G. Caldarelli, `cond-mat/0310503`
16. E. Almaas, B. Kovacs, T. Vicsek, Z.N. Oltvai, A.-L. Barabási, Nature (in press)
17. S. Redner, *A Guide to First-Passage Processes* (Cambridge University Press, USA, 2001)
18. S. Havlin, D. Ben-Avraham, Adv. Phys. **36**, 695 (1987)
19. M. Argollo de Menezes, A.-L. Barabási, to appear in Phys. Rev. Lett. `cond-mat/0306304`
20. S. Lawrence, L. Giles, Nature **400**, 107 (1999)
21. R. Albert, H. Jeong, A.-L. Barabási, Nature **401**, 130 (1999)
22. B. Kahng, Y. Park, H. Jeong, Phys. Rev. E **66**, 046107 (2002)
23. B. Tadic, Physica A **293**, 273 (2001)
24. A. Vazquez, R. Pastor-Satorras, A. Vespignani, Phys. Rev. E **65**, 066130 (2002)
25. S.-H. Yook, H. Jeong, A.-L. Barabási, Proc. Nat. Acad. Sci. **99**, 13382 (2002)
26. M. Barthélémy, B. Gondran, E. Guichard, Phys. Rev. E **66**, 056110 (2002)
27. K.A. Eriksen, I. Simonsen, S. Maslov, K. Sneppen, Phys. Rev. Lett. **90**, 148701 (2003)
28. R. Ferrer, C. Janssen, R.V. Solé, Phys. Rev. E **63**, 32767 (2001)
29. A.-L. Barabási, R. Albert, Science **286**, 509 (1999)
30. P. Erdös, A. Rényi, Publ. Math. Inst. Hung. Acad. Sci. **5**, 17 (1960)
31. A.-L. Barabási, H.E. Stanley *Fractal Concepts in Surface Growth* (Cambridge University Press, Cambridge, 1995)
32. *Dynamics of Fractal Surfaces*, edited F. Family, T. Vicsek (World Scientific, Singapore, 1991)
33. M. Argollo de Menezes, A. Vazquez, A.-L. Barabási, preparation
34. J.D. Noh, H. Rieger, `cond-mat/0307719 (2003)`
35. Y. Moreno, R. Pastor-Satorras, A. Vázquez, A. Vespignani, `cond-mat/0209474`
36. J. Hasty, J.J. Collins, Nat. Genet. **31**, 13 (2002)
37. N.S. Holter, A. Maritan, M. Cieplak, N. Fedoroff, J.R. Banavar, Proc. Natl. Acad. Sci. USA **98**, 1693 (2001)
38. H. Jeong, B. Tombor, R. Albert, Z.N. Oltvai, A.-L. Barabási, Nature **407**, 651 (2000)
39. H. Jeong, S. Mason, A.-L. Barabási, Z.N. Oltvai, Nature **411**, 41 (2001)
40. E. Ravasz, A.L. Somera, D.A. Mongru, Z.N. Oltvai, A.-L. Barabási, Science **297**, 1551 (2002)
41. R.N. Mantegna, H.E. Stanley, *An Introduction to Econophysics: Correlations and Complexity in Finance* (Cambridge Univ. Press, New York, 2000)
42. J.P. Bouchaud, M. Potters, *Theory of Financial Risk and Derivative Pricing: From Statistical Physics to Risk Management*, 2nd edn. (Cambridge University Press, USA, 2000)
43. L. Gillemot, J. Toyli, J. Kertesz, K. Kaski, Physica A **282**, 304 (2000)
44. J. Hasty, J. Pradines, M. Dolnik, J.J. Collins, Proc. Natl. Acad. Sci. USA **97**, 2075 (2000)
45. M.B Elowitz, A.J. Levine, E.D. Siggia, P.S. Swain, Science **297**, 1183 (2002)
46. M. Barthélémy, S.V. Buldyrev, S. Havlin, H.E. Stanley, Phys. Rev. E **61**, R3283 (2000)
47. L. de Arcangelis, S. Redner, A. Coniglio, Phys. Rev. B **34**, 4656 (1986)
48. J. Helsing, J. Axell, G. Grimvall, Phys. Rev. B **39**, 9231 (1989)
49. *Fractals in Science*, edited by A. Bunde, S. Havlin (Springer, Berlin, 1994)